DEVELOPMENT OF A 600 - 700 GHz SIS RECEIVER

W.R. McGrath[1], K. Jacobs[2], J. Stern[3], H.G. LeDuc[1], R.E. Miller[4], M.A. Frerking[1]

1. Jet Propulsion Laboratory, California Institute of Technology Pasadena, CA 91109
2. I. Physics Institute. University of Koeln, Koeln, West Germany
3. Physics Department, California Institute of Technology, Pasadena, CA
4. AT&T Bell Laboratories, Murray Hill, NJ 07974

Abstract

We report here on the development of a 600 - 700 GHz SIS receiver employing a waveguide mount designed to tune a large junction capacitance. A large scale model was used to optimize the bandwidth and tuning range of the mount. A new design of noncontacting backshort has been developed for use at 600 GHz. It performs as well as competing conventional designs at 100 GHz but is easily fabricated for use at submillimeter wave frequencies. NbN tunnel junctions are being developed for this receiver. We have made a systematic study of the mixer gain and noise of these junctions shunted with microstrip lines as rf tuning elements. This has given values of junction capacitance of 85fF/μ^2 and magnetic penetration depth of 3800Å. Mixer noise temperature as low as 134K has been achieved which is the best reported to date for an NbN junction.

Introduction

Many important chemical species in the interstellar medium, including HCl, H_2O, and CO, produce molecular line emissions in the 600 - 700 GHz frequency range. However, few observations presently exist due to the lack of sensitive heterodyne receivers. The nonlinear tunneling currents in an SIS tunnel junction provide the lowest noise mixing element in receivers at millimeter wavelengths (1-4). Theory suggests these receivers should provide exceptional performance up to the energy gap frequency of the superconductor comprising the tunnel junction. We report here on the development of a 600 - 700 GHz SIS receiver employing a waveguide mount designed to tune a large junction capacitance. Large scale model measurements of the mixer mount will be discussed. A new design of noncontacting waveguide backshort has been developed for use at submillimeter wave frequencies. It has performed well in tests up to 100GHz. Niobium nitride (NbN) tunnel junctions are being developed for this receiver. High quality NbN junctions with microstrip stubs have been fabricated and the mixer gain and noise performance studied at 200-210 GHz as a function of the inductance provided by the stub. This has yielded values for the junction capacitance and magnetic penetration depth. Mixer noise temperature as low as 134K has been obtained for properly tuned junctions. This is the best noise performance ever achieved for an NbN SIS mixer.

The Receiver

Figure 1 shows a block diagram of the receiver. The mixer mount, coupling mirror, and low-noise HEMT IF amplifier are housed in a LHe vacuum cryostat (5). The mixer and IF transformer are mounted to the LHe tank and are shrouded by a 20K radiation shield. Room temperature radiation in the optical path is reduced by cooled quartz and fluorogold far-IR filters. The signal and local oscillator are focussed onto the dual-mode conical feed horn of the waveguide mount by an off-axis mirror. This arrangement reduces standing waves which can become significant at these frequencies with conventional on-axis lenses.

The local oscillator (LO) power is generated by a Gunn oscillator operating at 105 GHz followed by a frequency doubler and tripler combination (6). The output power has been roughly measured at 40μW. This is sufficient power to properly to drive the SIS mixer. The Gunn oscillator frequency is stabilized to better than 2 parts in 10^8 by a phase lock system. The signal and local oscillator (LO) source will be diplexed using either a Mach-Zehnder interferometer or a simple mylar beamsplitter, depending on the strength of the LO source and the rf coupling efficiency of the mixer mount. The interferometer gives a low LO transmission loss, however our experience with 205 GHz SIS mixers (7) suggests that a 95% beamsplitter may be sufficient.

The receiver is calibrated by chopping between ambient temperature and cold (77K) blackbodies made from Eccosorb. The receiver gain and noise can thus be measured for each spectral channel. The sky temperature is then measured by chopping the sky against the cold blackbody.

The IF output power from the mixer is coupled to the low noise IF system by a microstrip impedance transformer. Excellent coupling efficiency to the 50Ω IF system with sufficient bandwidth can be achieved with properly optimized transformers. The first stage of the IF system is a cooled HEMT amplifier with a bandwidth of 1.1 - 1.7 GHz, a gain of 33dB, and a noise temperature about 6K. Room temperature amplifiers are then used to obtain sufficient power to drive an acousto-optic spectrometer.

The SIS Mixer Mount

An important figure of merit for an SIS tunnel junction is the relaxation parameter ωRC where ω is the angular frequency, R is the junction resistance, and C is the junction capacitance. Experimentally it has been found (1) that best results are usually obtained for ωRC > 1, which implies a large junction capacitance which must be properly tuned by the mixer mount. We have chosen a waveguide mount with an adjustable backshort and E-plane tuner in order to accomodate large values of ωRC. A 130X

scale model of this mount is used in conjunction with a 3-6 GHz network analyzer to optimize the mount design (8). The effects on the rf tuning range produced by the size of the coupling hole in the waveguide broad wall, the size of the substrate, and the shape of the rf filter metallization have been studied. In addition, a 2000X scale model of the SIS junction with an integrated microstrip line as a tuning element has also been investigated.

Figure 2 shows a photo of the large scale model. The model waveguide dimensions are 47.5mm x 22.1mm. The mixer block is split along the center of the waveguide broadwall to simplify the machining and construction. A symmetrical channel 17mm wide x 9.5mm deep is cut in each half of the block to hold the junction substrate which is 14.3mm wide x 7mm thick. These substrate dimensions were chosen to correspond to 0.11mm x 0.054mm in the actual mixer. Thinner substrates would become increasingly difficult to fabricate and handle. The substrate is in the E-field direction with the junction metallization parallel to the narrow wall of the waveguide. A microstrip rf filter was designed to provide a short circuit at the wall where the substrate enters the waveguide. The length of the first filter sections were subsequently adjusted to optimize the tuning range of the mount. A 0.86mm diameter coaxial cable was soldered to the rf filter metallization and used to sample the mount impedance at the position of the junction. The E-plane tuner is located about one guide wavelength in front of the junction at 4.8GHz (corresponding to 624GHz in the final mixer).

This mount configuration gives an acceptably broad range of imbedding impedances from 4.55 GHZ to 5.30 GHZ (593GHz to 690GHz). Just above or below these frequencies, the range of impedances shrinks to an unacceptably small region of the Smith chart, but only over a narrow range of frequencies. This effect is related, at least in part, to the large hole in the waveguide produced by the substrate channel. Decreasing the depth of the channel in one half of the block to 6mm extended the acceptable tuning range to 5.57GHz (725GHz). Also, reducing the substrate width to 11.4 mm increased the range of accessible impedances at 5.57GHz. Thus the tunable bandwidth of this mount is about 20%.

This is sufficiently broad as it greatly exceeds the tuning range of the LO sources at these frequencies.

The rf filter metallization must taper down to the junction area. The angle of this taper was found to affect the size of the forbidden tuning region (9). A 90° taper produced a large forbidden region centered 35° above the real axis and encompassing real impedances from 38Ω to 1000Ω at 4.8 GHz(624GHz). A 45° taper significantly reduced the size of the forbidden region and rotated it clockwise around the Smith chart. The shaded area in Fig. 3 shows the final tuning range obtained for the mount. RF junction resistance as low as 5Ω and $\omega RC < 6$ for R=50Ω can be tuned.

Figure 4 shows a photo of one half of the mixer block. The waveguides are cut with conventional machining techniques and then polished to the final dimensions 0.366mm wide x 0.170mm high. This gives a fundamental mode waveguide band of 410GHz - 820GHz. Radiation is coupled into the mixer block with a dual mode conical horn. These horns are fabricated using an electroform technique and their properties have been previously reported (10). The far-field pattern has a 3dB half angle of 6° which allows for easy coupling to telescope feed optics.

New Backshort Design

Contacting backshorts are normally used at these high frequencies due to the very small dimensions of the waveguides. Figure 5(a) shows a conventional contacting backshort. The contact area is critical and must make good contact to produce an acceptable short circuit. These backshorts are excellent in that they provide a short circuit over the entire waveguide band. However, the contacting areas can eventually degrade from sliding friction. It is also difficult to get a uniform contact with the waveguide walls at high frequencies where the waveguide dimensions become fractions of a millimeter.

Another approach commonly used is the noncontacting backshort shown in Fig. 5(b). A thin mylar insulator prevents contact and allows the backshort to slide smoothly. In order to produce an rf short circuit, and hence a large reflection, this backshort has a

series of high impedance and low impedance sections which are usually $\lambda_g/8$ to $\lambda_g/4$ in length (where λ_g is the guide wavelength). However, at very high frequencies the thin high impedance sections become too thin to easily fabricate and the backshort is no longer strong enough to slide snugly in the waveguide. An alternative approach is needed.

A new noncontacting backshort design has been developed (11) and is shown in Fig. 6. In order to obtain a large reflection, a noncontacting backshort must provide a periodic variation of guide impedance on the correct length scale. This is accomplished in the new design by either rectangular or circular holes with the proper dimension and spacing cut into a metallic bar. This bar is dimensioned to form a snug fit in the waveguide with a mylar insulator. The holes replace the thin high impedance sections in the conventional design shown in Fig. 5(b). The new design is easy to fabricate and can be used at any waveguide frequency between 1GHz and 1000GHz. For very high frequencies, above a few hundred GHz, the metallic bar is a piece of shim stock polished to the correct thickness. The holes can be formed by drilling, punching, or can be etched using common fabrication techniques.

Several backshorts were built and tested at 3.1-6.2 GHz and 75-115 GHz with a variety of hole sizes and spacings. Figure 7 shows the reflection for a backshort with rectangular holes. The reflection coefficient is > 0.99 over a 40% bandwidth. This is as good as a conventional backshort. The center frequency is estimated to be 3.87GHz. This implies the high impedance section lengths are $0.16\lambda_g$ and the low impedance section lengths are $0.14\lambda_g$. The presence of the mylar modifies the waveguide modes. The guide wavelengths, λ_g, for the high and low impedance sections were estimated using an approach outlined in references 12 and 13. Figure 8 shows the reflection for a backshort with three circular holes. The reflection is >0.99 over a 26% bandwidth with a center frequency of 4.3 GHz. As can be seen in both of these figures, there are regions of reduced reflection at either the high or low end of the frequency range. These result

from power which leaks through the short due to the complex mode structure produced by the holes.

In order to test if the designs could be scaled to millimeter wave frequencies, a backshort with rectangular holes was fabricated for 75-115 GHz. The results are shown in Fig. 9. As can be seen, this figure is similar to Fig. 7 which implies the design can be scaled to high frequencies.

SIS Junctions

This receiver system will use either Pb-alloy tunnel junctions produced at AT&T Bell Laboratories or NbN-MgO-NbN junctions produced at JPL. It is desirable to use integrated tuning elements with the junctions to resonate out the junction capacitance over a broad bandwidth. We have chosen an open-circuited microstrip stub to provide an inductive susceptance (14). Figure 10 shows the suspended photoresist bridge technique used to produce the Pb-alloy junctions. Since a microstrip stub cannot be easily added after the junction fabrication steps, we have developed the geometry shown in fig. 11. The center conductor is put down first on the substrate. This is covered by an SiO layer, and then the junction and rf filter layer are deposited last to form the ground plane for the line.

A 2000x scale model of this geometry has been investigated. Plane A is the reference plane for the stub. The length of center conductor from A to B forms an inductance L_1 and the rf filter metallization from B to the junction completes the circuit with an inductance L_2. These inductances to good approximation add directly to the inductance L_t of the stub to resonate with the junction capacitance. Figure 12 shows the equivalent circuit. At resonance the real part of the junction impedance is reduced by the factor $n = (L_1+L_t \; / \; L_1+L_2+L_t)^2$. We estimate L_1 =1.4pH and L_2 = 0.6pH for a 5μ wide stub and A-to-B distance of 5μ. This yields typically n = 0.5 - 0.7 depending on junction capacitance and hence L_t. Model measurements at 312 MHz confirm the effect of L_1 and L_2 on the resonant frequency and the value of n. These results indicate that at frequencies near 600GHz, micron scale

features near the junction must be properly included in the rf circuit.

All niobium nitride (NbN) tunnel junctions with MgO barriers are being fabricated at JPL (15). NbN is a chemically stable and mechanically rugged refractory metal which makes it well suited for practical receiver applications. In addition, the high energy gap of 5 mV will allow for operation near 1000GHz and for easier descrimination against interferring Josephson effects. However, the high specific capacitance of these junctions is best tuned with a microstrip stub. Proper design of the stub requires accurate knowledge of the junction capacitance and the magnetic penetration depth in the superconducting film. These parameters are well known for the extensively developed Pb-alloy junctions, but are less accurately known for the new NbN junctions. We have fabricated high quality NbN junctions with microstrip stubs and studied the mixer gain and noise performance at 200-210 GHz as a function of the inductance provided by the stub. This has yielded values for the junction capacitance and magnetic penetration depth.

The phase velocity in the stub determines the length and is calculated using the expression (14)

$$\upsilon/c = (\varepsilon_r (t_d + \lambda_1 \coth(t_1/\lambda_1) + \lambda_2 \coth(t_2/\lambda_2)) / t_d << 1 \quad (1)$$

where ε_r is the dielectric constant, t_d is the dielectric thickness, λ_1 and λ_2 are the magnetric penetration depths in the top and bottom electrodes respectively, and t_1 and t_2 are the thicknesses of the top and bottom elecrodes respectively. For our stubs, the magnetic penetration depth (3000Å - 4000Å), the film thickness (3000Å), and the dielectric thickness (1500Å) are comparable. In this case, υ and hence the resonant frequency are sensitive to λ. Thus λ must be accurately known to properly design the resonant circuit.

Small area, high current density NbN-MgO-NbN tunnel junctions are fabricated using a recently developed trilayer process which

is fully described elsewhere (15). The junctions have an area 1x1 μ^2, a current density J_c = 5000 - 10,000 A/cm^2, and a normal state resistance R_n = 50-70Ω. The gap voltage is V_g = 4.8 mV at 4.2K, and the width ΔVg of the quasiparticle current rise at V_g is typically about 1 mV. This is slightly larger than the characteristic photon voltage of 0.875 mV at 205 GHz. Figure 13 shows a typical I-V curve.

Each junction was fabricated with a microstrip stub. Stubs 75μ, 80μ, and 86μ long by 4.5μ wide, and 75μ by 7μ were tested. The total capacitance each stub would resonate with is calculated using $C = 1/(\omega^2 L)$ where L is the stub inductance.

Accurate measurements of mixer gain and noise are required to properly characterize the rf effects of the stubs. We have built a specially designed test system to perform these measurements. Figure 14 shows a block diagram of the mixer test system which is mounted in a commercial vacuum cryostat. It employs variable-temperature blackbodies (loads) at the rf input and IF output of the mixer. The novel feature is the IF load (16) which is cryogenically-coolable and is placed in the cryostat close to the mixer thus minimizing errors due to transmission line losses. Mixer gain and noise temperature can be measured to better than ±8%. These measured values include the small losses due to the LO diplexer, mylar vacuum window, and fluorogold IR filter for the current NbN mixer tests. The mixer block is a full height waveguide mount (17) employing a noncontacting backshort and E-plane tuner. Due to the low LO power requirements, a simple mylar beamsplitter is used to reflect about 2% of the incident LO power into the cryostat. The LO source consists of a 68GHz Gunn oscillator driving a x3 frequency multiplier which employs a whisker contacted Schottky barrier diode. A similar arrangement is used to provide monochromatic signals to optimize the mixer.

A cooled coaxial switch allows power from either the mixer or IF load to enter the IF system. A 20dB bidirectional coupler allows test signals to be injected for evaluating the mixer IF mismatch and the IF system gain. A cooled isolater is used to minimize the effects of impedance changes on the noise of the IF

system. The first gain stage is provided by a HEMT amplifier with a gain of 38dB and a noise temperature of 6K. Room temperature bandpass filters with a center frequency of 1.4 GHz and a bandwidth of 100 MHz are used for the noise measurements.

Using high quality Pb-alloy SIS tunnel junctions, this mixer test system has given overall double-sideband receiver noise temperatures as low as 113K (7). This is comparable to the performance reported for fully optimized receivers in this frequency range (3,17,18).

Mixer Performance of NbN Junctions

Figure 15 shows the mixer noise temperature versus the capacitance tuned by the stub. Without a stub, values above 1000K were obtained. However, T_m below 200K was obtained for stubs which tuned a capacitance near 85fF which agrees well with previously reported data (19) using a SQUID interferometer technique. Mixer gain was also found to improve from -19dB without a stub to -11dB with one.

Figure 16 shows mixer noise temperature versus frequency at 4.2K and 1.5K. The best result is T_m = 134K at 202.5 GHz. Mixer noise improved by about 50K on cooling the junction to 1.5K. The mixer gain also improved by 2-3dB. Mixer performance is expected to change with changes in the shape of the I-V curve (20). In these junctions, ΔV_g showed almost no change, and the subgap current decreased 10% - 50% depending on bias voltage. A decrease in subgap current could improve mixer noise but may not fully account for the improvements in mixer gain. Detailed calculations with Tucker's quantum mixer theory (21) are required to fully interpret changes in the I-V curve.

Another possibility is ac losses in the superconductive stubs. Kautz (22) has published calculations for losses in superconductive microstrip and shown that these losses can be strongly temperature dependent even below half the superconducting transition temperature. Since the Q of our stub tuned junctions is relatively high, about 8, even a small loss would strongly affect the performance. Using a simple lumped element model of the junction shunted with a lossey microstrip

stub, we calculate that resistance of 2-5Ω would degrade the mixer return loss to less than 10dB. Figure 17 shows the results. We are currently investigating the losses in our microstrip lines.

The propagation velocity υ on the stub was determined by a method (14) using the ac Josephson effect in the junction as a voltage controlled oscillator to sample the resonances of the circuit. The frequency spacing of these resonances is given by $\upsilon/2l$ where l is the length of the stub. This method gave λ = 3800Å for our films, which is significantly larger than the previously reported value of 2800Å (19). This led to stub lengths of 75-80μ for best mixer performance.

Summary

A 600-700 GHz SIS receiver employing a waveguide mount is being developed. A large scale model was used to optimize the bandwidth and tuning range of the mount. A new design of noncontacting backshort has been developed for use at 600 GHz. It performs as well as competing conventional designs at 100 GHz but is easily fabricated for use at submillimeter wave frequencies. NbN tunnel junctions are being developed for this receiver. We have made a systematic study of the mixer gain and noise of these junctions shunted with microstrip lines as rf tuning elements. This has given values of junction capacitance of 85fF/μ^2 and magnetic penetration depth of 3800Å. Mixer noise temperature as low as 134K has been achieved which is the best reported to date for an NbN junction.

Acknowledgements

This work was supported in part by the Jet Propulsion Laboratory, California Institute of Technology under contract with the National Aeronautics and Space Administration, and the Strategic Defense Initiative Organization.

References

1. Tucker, J. R. and Feldman, M. J. *Rev. Mod Phys.*, **57**, p. 1055 (1985).

2. Pan, S.-K.; Kerr, A. R.; Feldman, M. J.; Kleinsasser, A. W.; Stasiak, J. W.; Sandstrom, R. L.; Gallagher, W. J. *IEEE Trans. Microwave Theory Tech.*, **MTT-39**, 580 (1989).

3. Blundell, R.; Carter, M.; Gundlach, K. H. *Int. J. IR & mm Waves*, **9**, p. 361 (1988).

4. Buttgenbach, T. H.; Miller, R. E.; Wengler, J. J.; Watson, D. M.; Phillips, T. G. *IEEE Trans. Microwave Theory Tech.*, **MTT-36**, 1720 (1988).

5. Ellison, B. N. *Cryogenics*, **28**, 779 (1988).

6. The local oscillator source was developed at Radiometer Physics, Bonn, West Germany under contract to the Jet Propulsion Laboratory.

7. McGrath, W. R.; Byrom, C. N.; Ellison, B. N.; Frerking, M. A.; Miller, R. E. *Digest 13th Int. Conf. Infrared and Millimeter Waves*, p. 98 (1988).

8. Jacobs, K. A.; McGrath, W. R. *Digest 14th. Int. Conf. Infrared and Millimeter Waves*, p. 540 (1989).

9. Collins, R.E. *Foundations for Microwave Engineering*, McGraw-Hill (1966).

10. Pickett, H. M.; Hardy, J. C.; Farhoomard, J. *IEEE Trans. Microwave Theory Tech.*, **MTT-32**, p. 936 (1984).

11. McGrath, W. R., Jet Propulsion Laboratory, Notice of New Technology Case No. JPL I.R. 30-18091/7600 (1990).

12. Brewer, M. K. and Raisanen, A. V. *IEEE Trans. Microwave Theory Tech.*, **MTT-30**, 708 (1982).

13. Harrigton, R. F. *Time-Harmonic Electromagnetic Fields*, McGraw-Hill, pp. 158-161 (1961).

14. Raisanen, A. V.; McGrath, W. R.; Richards, P. L.; Lloyd, F. L. *IEEE Trans. Microwve Theory Tech.*, **MTT-33**, p. 1495 (1985).

15. Stern, J. A.; Hunt, B. D.; LeDuc, H. G.; Judas, A.; McGrath, W. R.; Cypher, S. R.; Khanna, S. K. *IEEE Trans. Magn.*, **MAG-25**, p. 1054 (1989).

16. McGrath, W. R.; Raisanen, A. V.; Richards, P. L. Int. J. IR & mm Waves, **7**, p. 543 (1986).

17. Ellison, B. N.; Miller, R. E. *Int. J. IR & mm Waves*, **8**, 608 (1987).

18. Woody, D. G.; Giovanine, C. J.; Miller, R. E. *IEEE Trans. Magn*, **MAG-25**, p. 1366 (1989).

19. Shoji, A.; Aoyagi, M.; Kosaka, S.; Shinoki, F.; Hayakawa, H. *Appl. Phys. Lett.*, **46**, p. 1098 (1985).

20. McGrath, W. R.; Richards, P. L.; Face, D. W.; Prober, D.; Lloyd, F. L. *J. Appl. Phys.*, **63**, p. 2479 (1988).

21. Tucker, J. R. *IEEE J. Quantum Elec.*, **QE-15**, 1234 (1978).

22. Kautz, R. *J. Appl. Phys.*, **49**, 308 (1978).

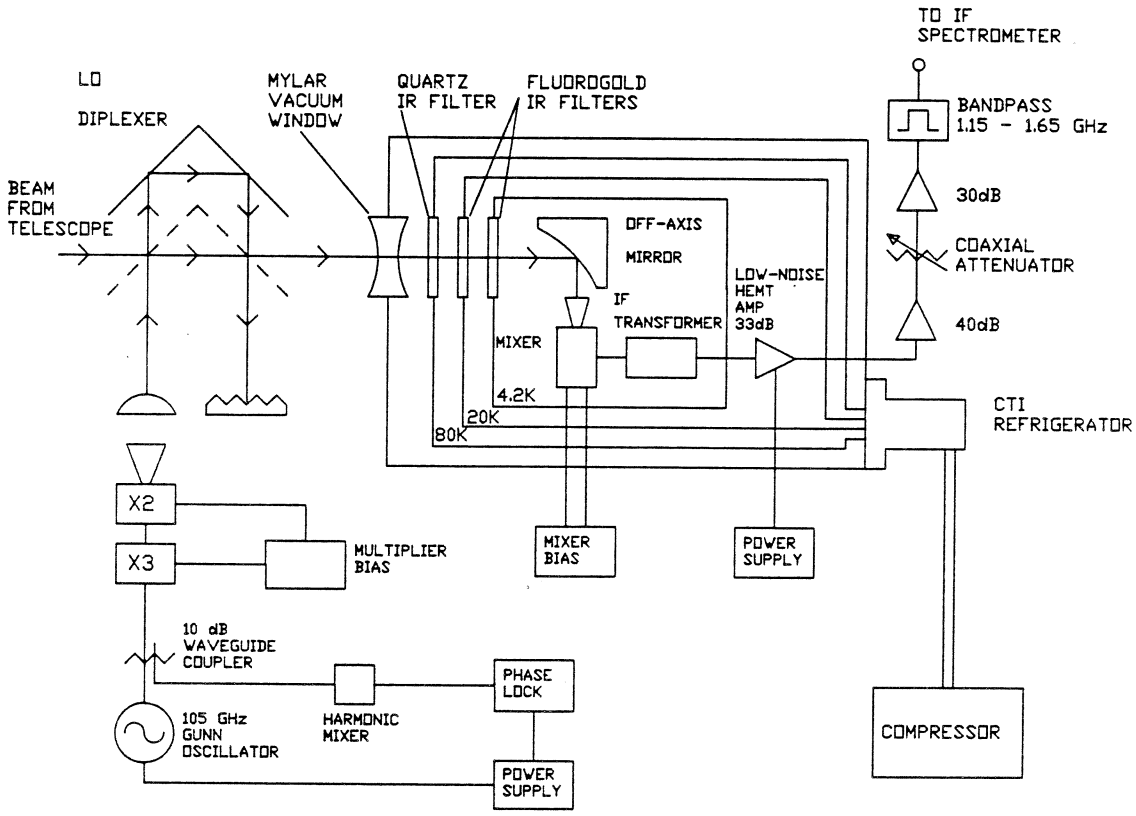

Fig.1 Block diagram of 600-700GHz SIS receiver.

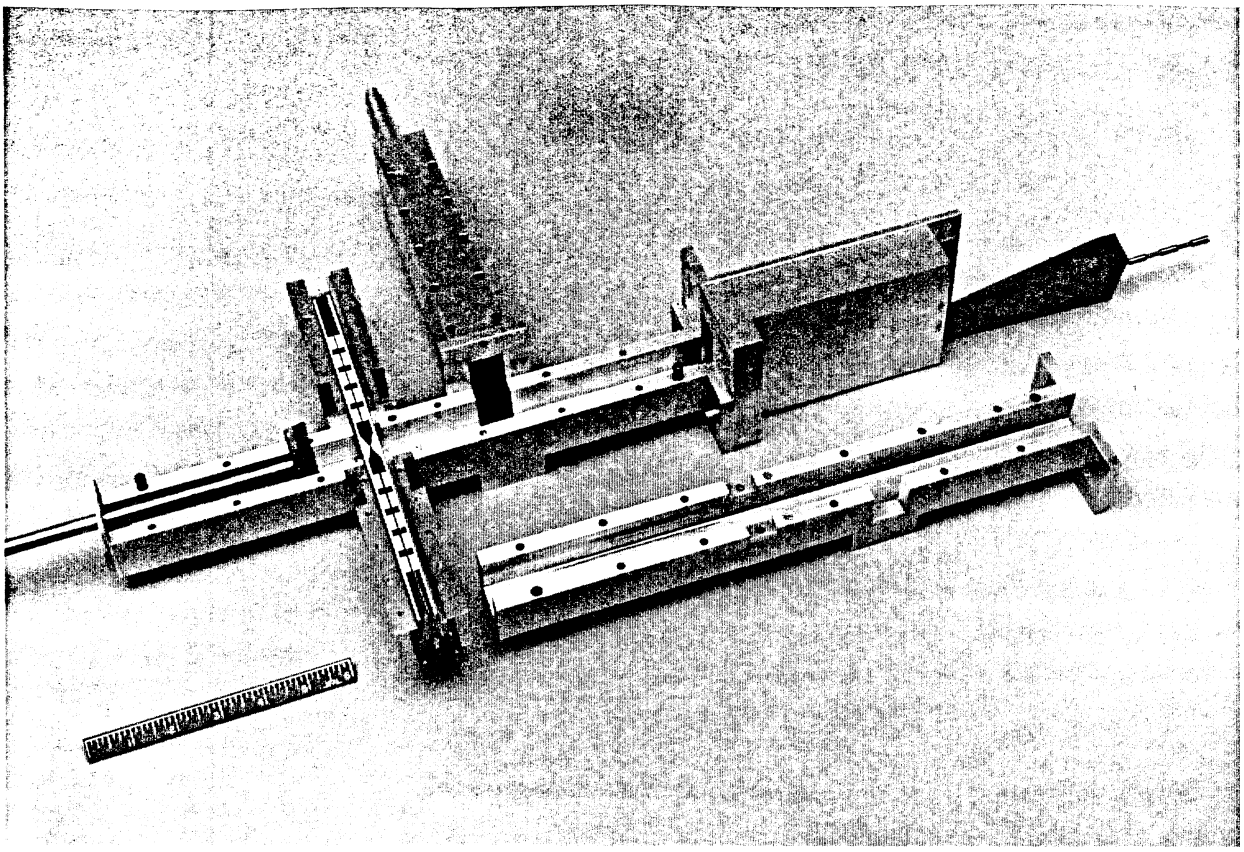

Fig.2 Large scale, 3-6GHz model of waveguide SIS mixer mount.

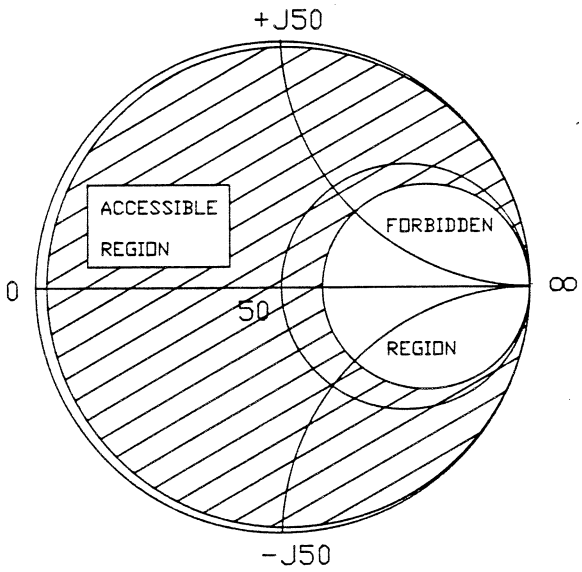

Fig.3 Impedance Smith Chart showing tuning range of mixer mount.

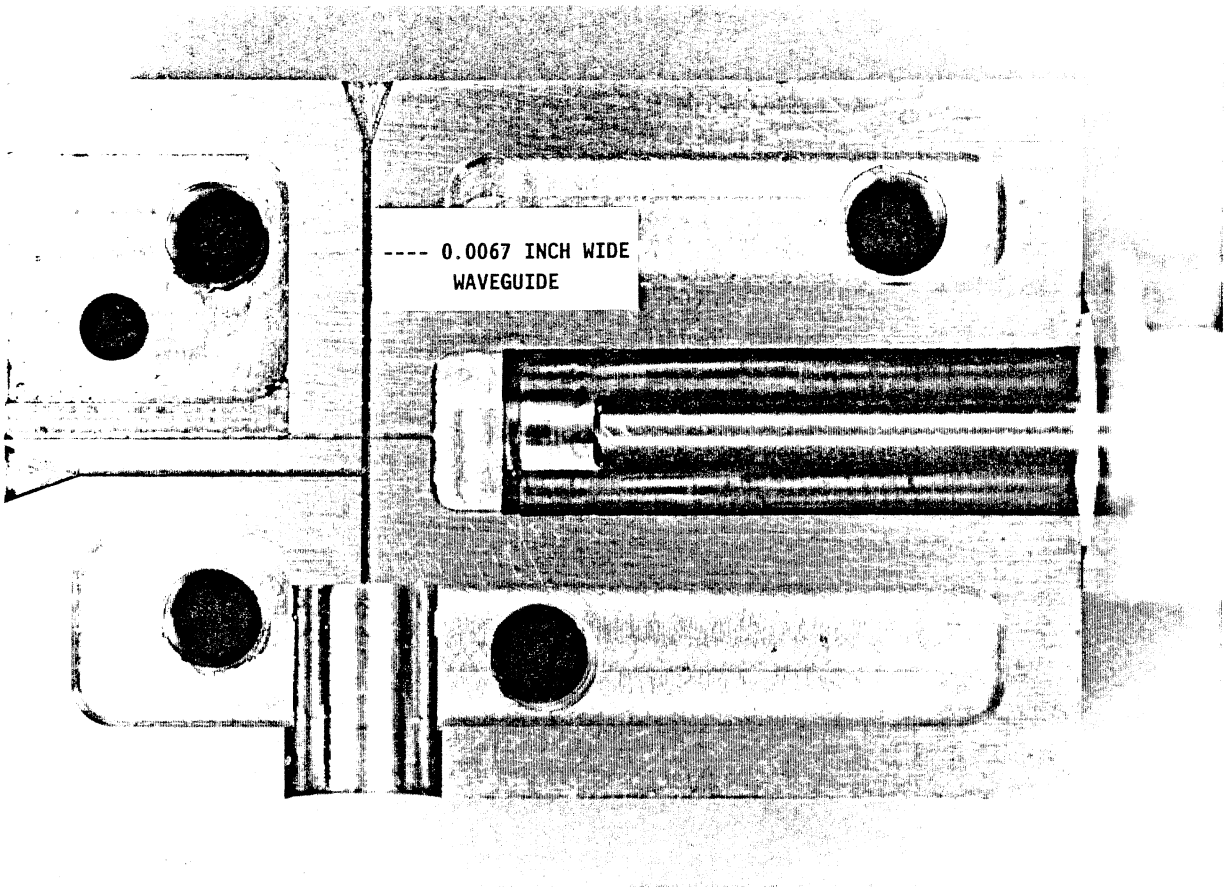

Fig.4 Photo of one half of mixer block. The waveguides are flared at the ends to assist insertion of backshorts. The conical horn fits into the cylindrical cavity at the lower end of the main waveguide.

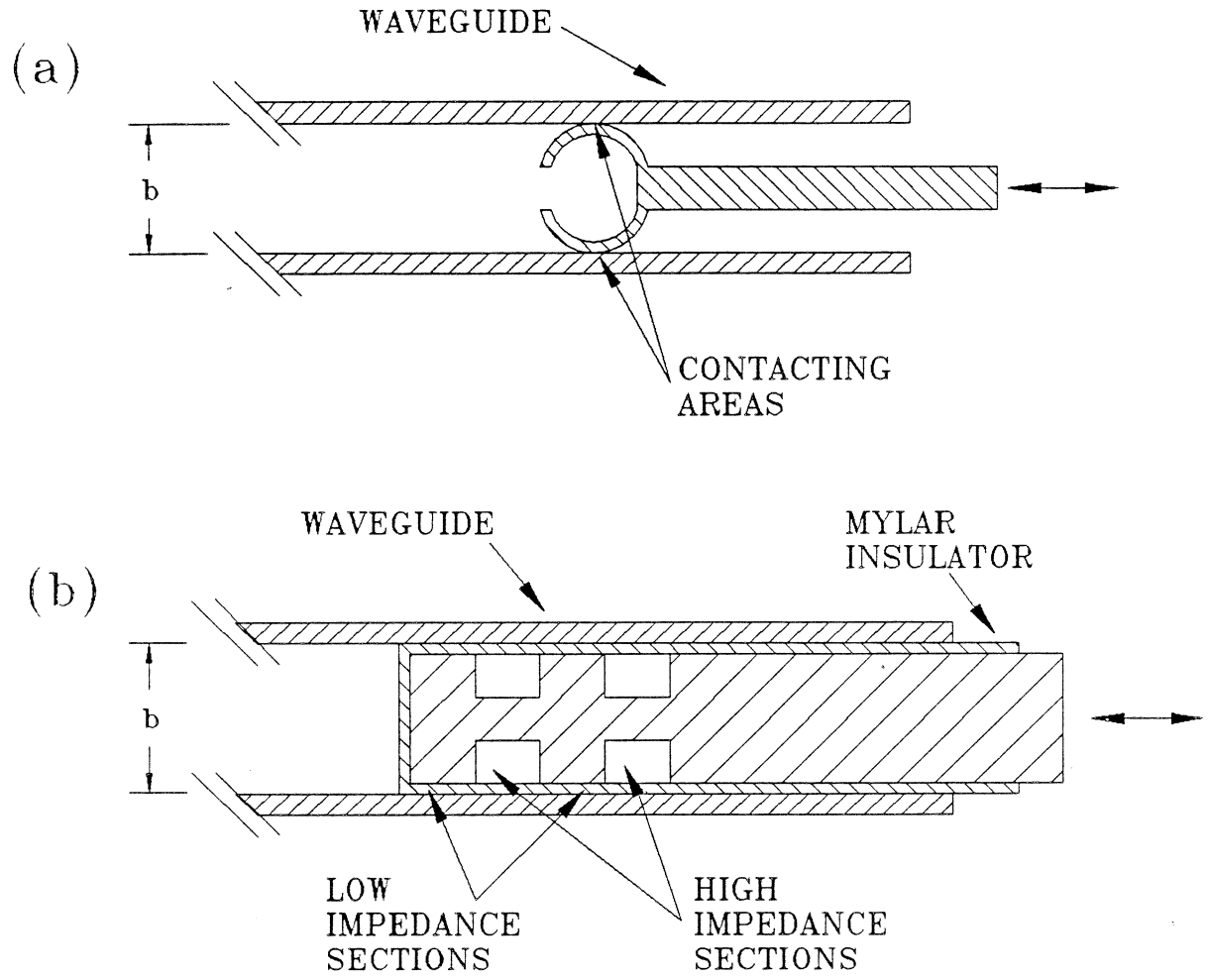

Fig.5 Schematic diagram of conventional backshort designs. (a) contacting backshort; (b)noncontacting backshort.

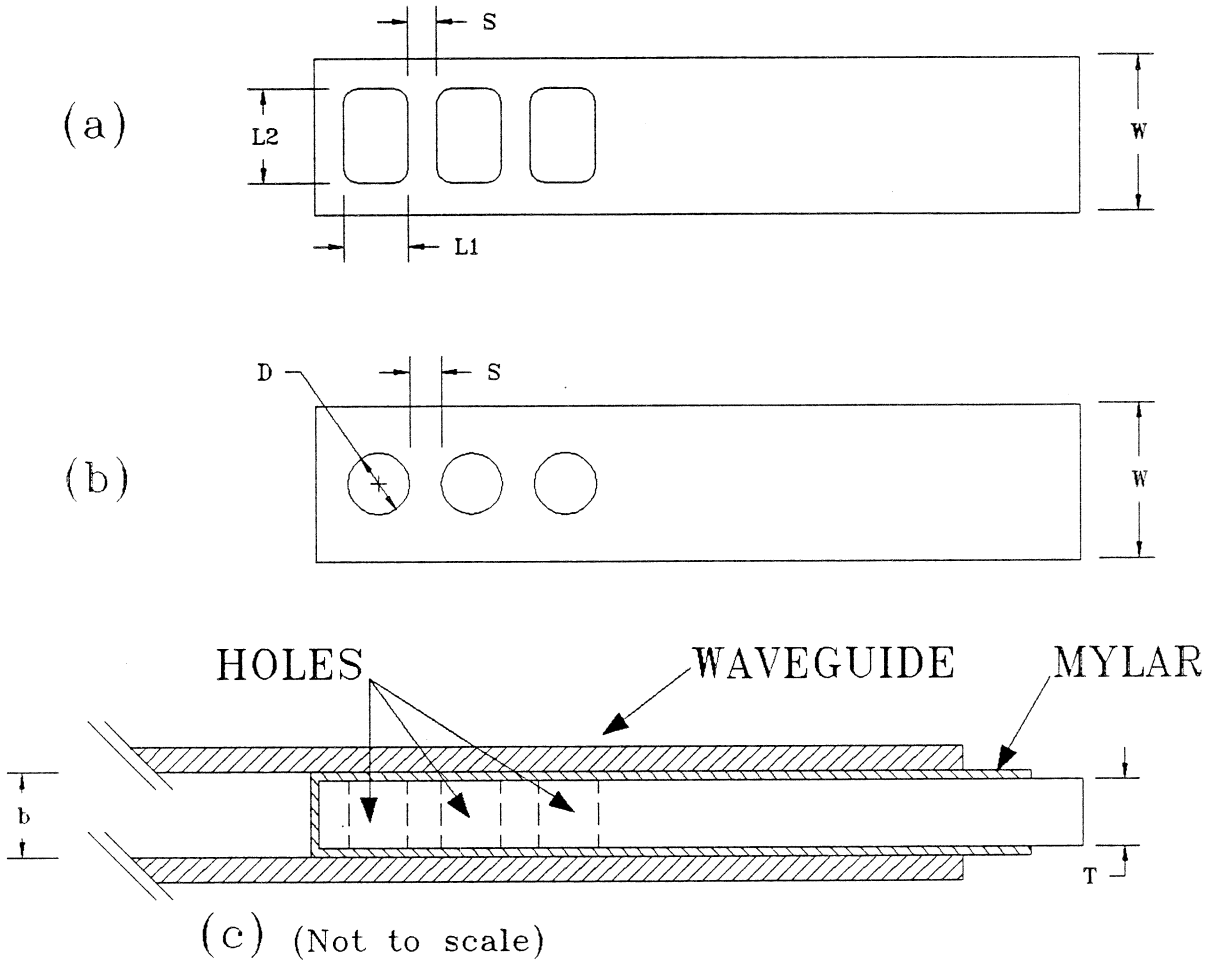

Fig.6 New backshort design employing (a) rectangular or (b) circular holes to provide the proper impedance variation for a large reflection. (c) Cross sectional view in waveguide.

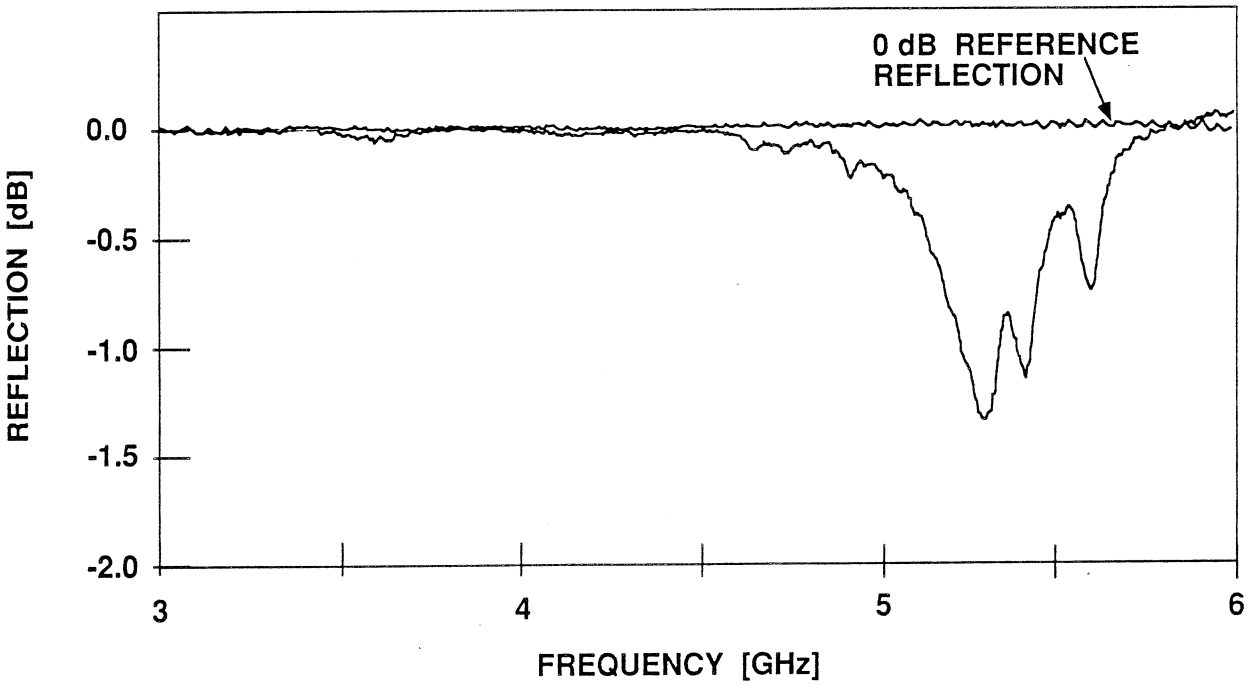

Fig.7 Reflection from model backshort with 3 rectangular holes.

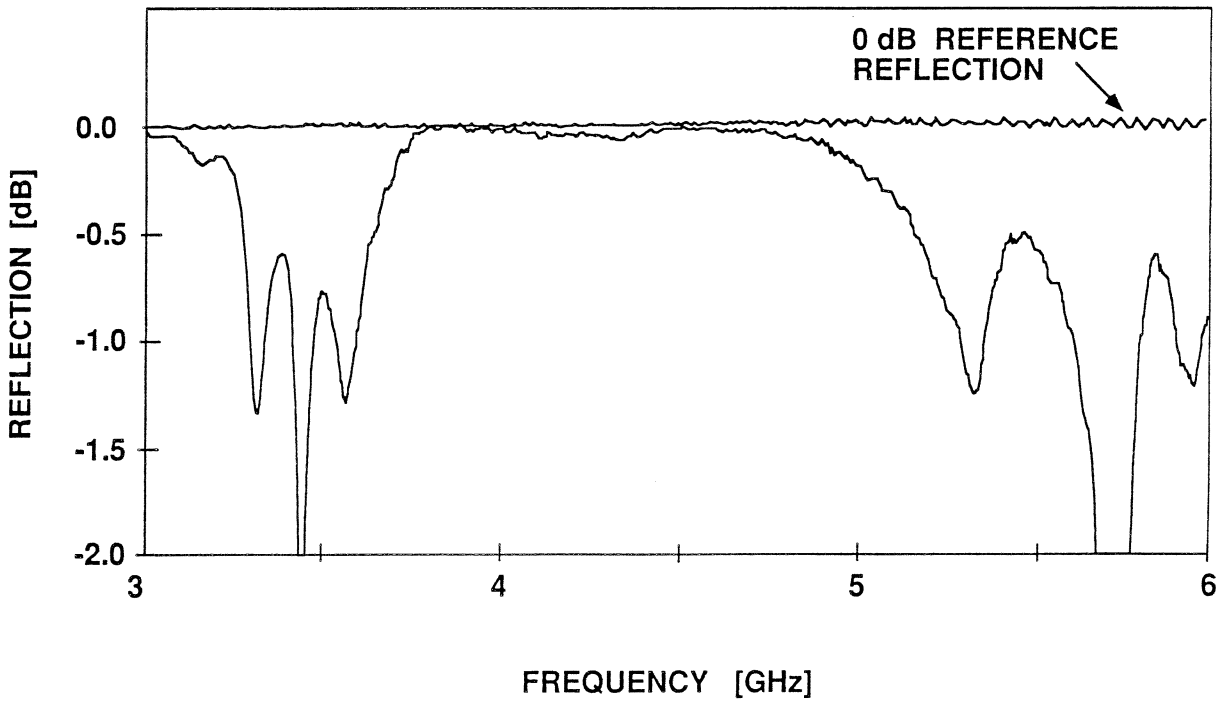

Fig.8 Reflection from model backshort with 3 circular holes.

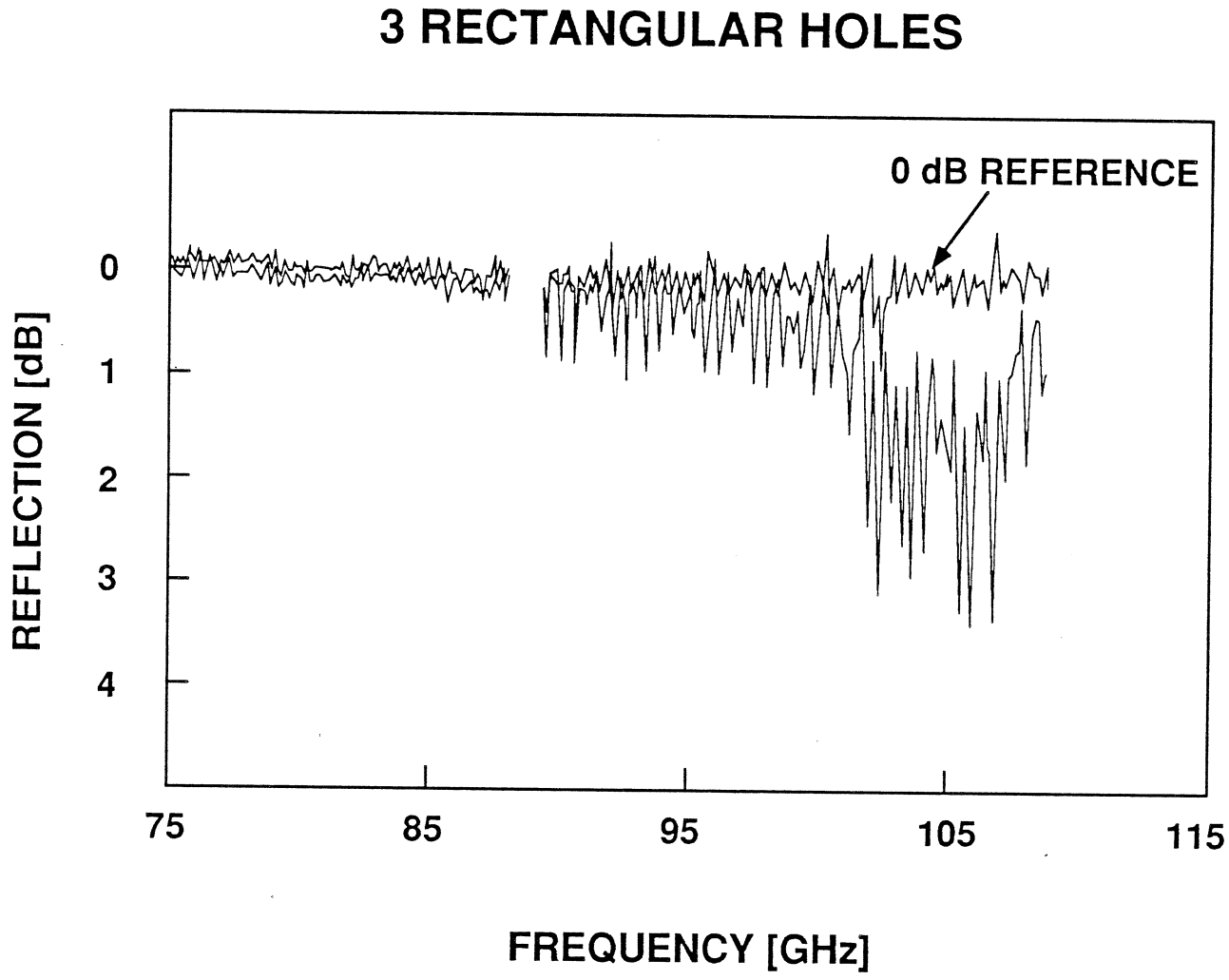

Fig.9 Reflection from millimeter wave backshort with rectangular holes.

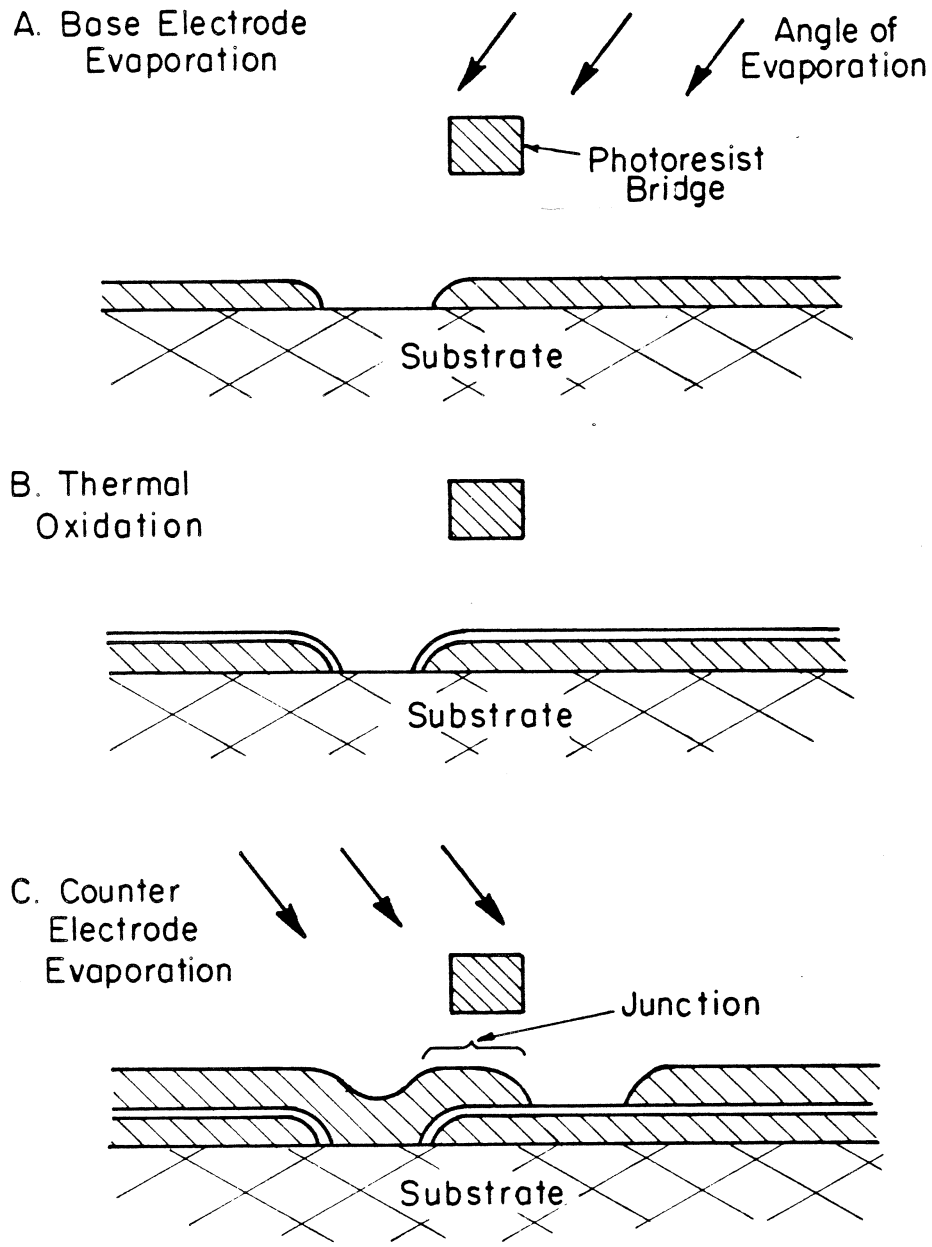

Fig.10 Fabrication of Pb-alloy tunnel junctions using photoresist bridge technique.

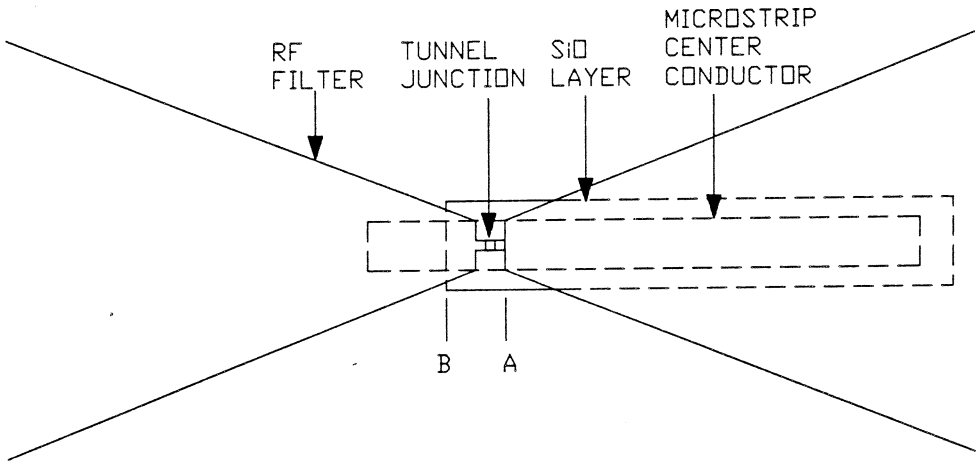

Fig.11 Diagram of microstrip tuning stub integrated with Pb-alloy junction.

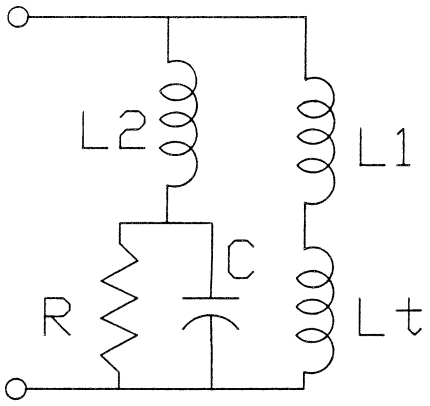

$L1+L2+Lt$ RESONATE WITH C

$Rrf = nR$

$n = (L1+Lt/L1+L2+Lt)^2 = 0.5-0.7$

Fig.12 Equivalent circuit of stub tuned junction.

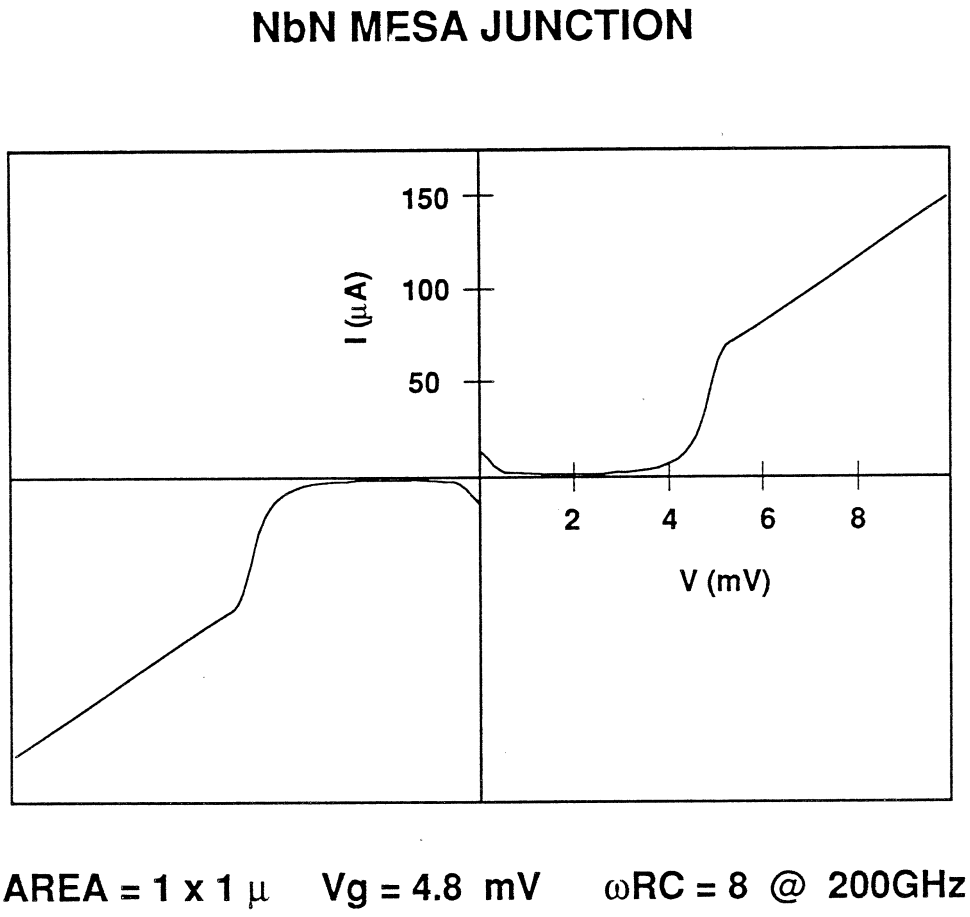

Fig.13 Typical I-V curve for NbN-MgO-NbN tunnel junction.

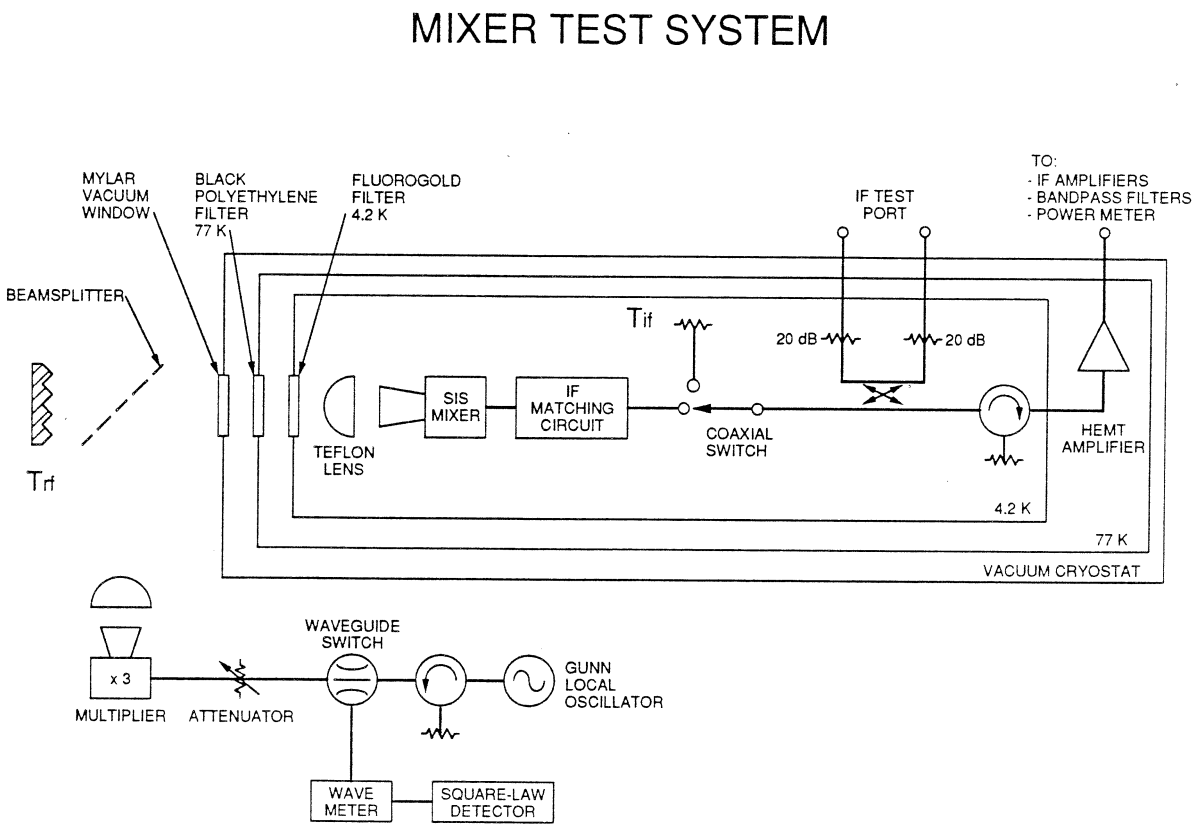

Fig.14 Test system employing cooled IF load to characterize mixer performance.

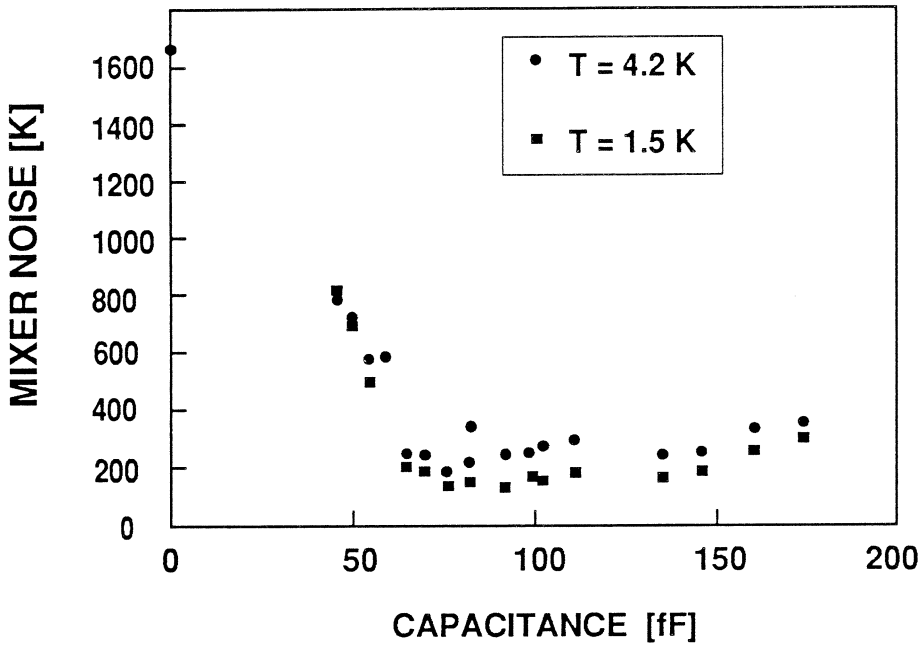

Fig.15 Mixer noise temperature versus capacitance tuned by the microstrip stub.

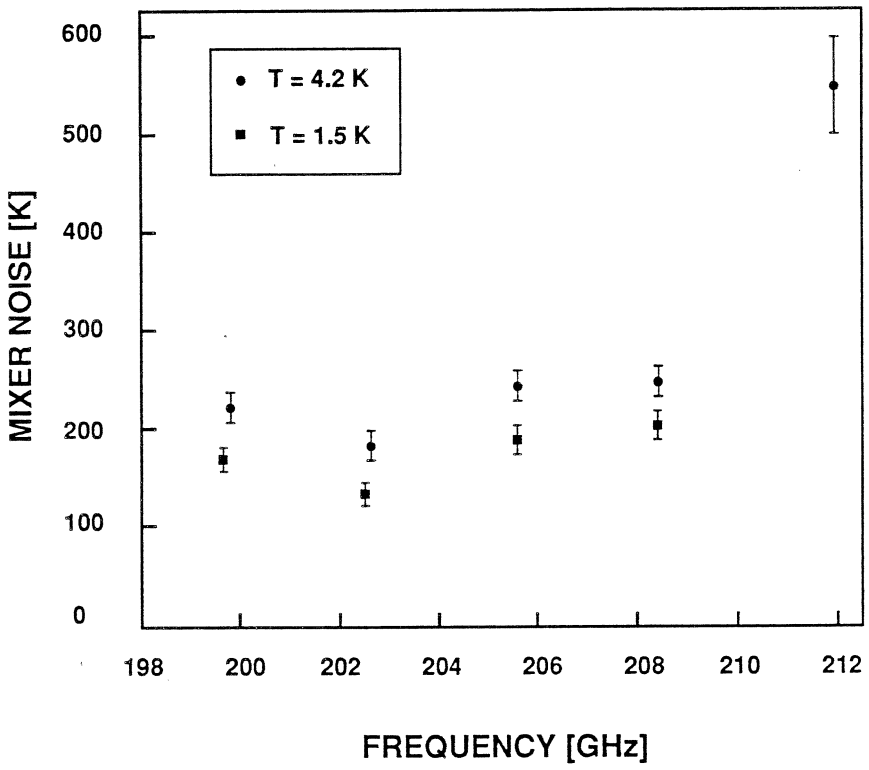

Fig.16 Mixer noise temperature versus frequency at two physical temperatures: 1.5K and 4.2K.

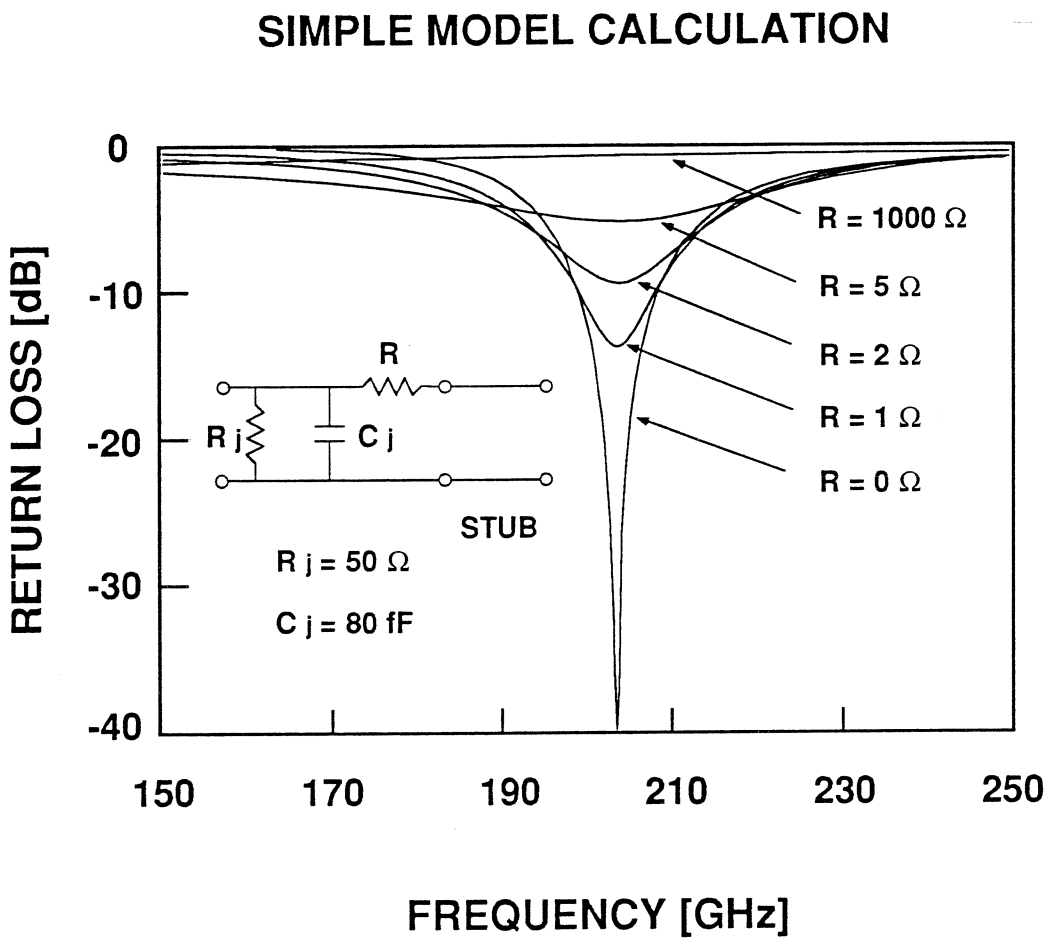

Fig.17 Simple calculation of the effect of loss in the stub on mixer rf coupling.